Treatment of Observation Error due to Unresolved Scales in Atmospheric Data Assimilation

TIJANA JANJIĆ*

School of Engineering and Science, International University Bremen, Bremen, Germany

STEPHEN E. COHN

Global Modeling and Assimilation Office, NASA Goddard Space Flight Center, Greenbelt, Maryland

(Manuscript received 28 February 2005, in final form 19 January 2006)

ABSTRACT

Observations of the atmospheric state include scales of motion that are not resolved by numerical models into which the observed data are assimilated. The resulting observation error due to unresolved scales, part of the "representativeness error," is state dependent and correlated in time. A mathematical formalism and algorithmic approach has been developed for treating this error in the data assimilation process, under an assumption that there is no model error. The approach is based on approximating the continuum Kalman filter in such a way as to maintain terms that account for the observation error due to unresolved scales. The two resulting approximate filters resemble the Schmidt–Kalman filter and the traditional discrete Kalman filter.

The approach is tested for the model problem of a passive tracer undergoing advection in a shear flow on the sphere. The state contains infinitely many spherical harmonics, with a nonstationary spectrum, and the problem is to estimate the projection of this state onto a finite spherical harmonic expansion, using observations of the full state. Numerical experiments demonstrate that approximate filters work well for the model problem provided that the exact covariance function of the unresolved scales is known. The traditional filter is more convenient in practice since it requires only the covariance matrix obtained by evaluating this covariance function at the observation points. A method for modeling this covariance matrix in the traditional filter is successful for the model problem.

1. Introduction

Measurements of atmospheric variables are made at various times and at various locations using instruments that are accurate to within some tolerance called the measurement (or instrument) error (e.g., Daley 1991; Atlas 1997; Rodgers 2000). In the context of data assimilation there is, in addition to the measurement error, a "representativeness error" that arises from the variability of the observed field at scales smaller than those resolved by the assimilating dynamical model, and from the discrete approximation of the exact, continuum observation operator (Lorenc 1986; Cohn 1997). For observations of highly variable fields such as wind, moisture, and trace constituents, the representativeness error can be considerably larger than the measurement error (e.g., Ménard et al. 2000).

Proper treatment of representativeness error in the data assimilation process is complicated by the fact that it is state dependent and correlated in time (Daley 1992; Mitchell and Daley 1997a,b). Even if the state dependence and time correlation are neglected, one must still specify a representativeness error covariance matrix. To gain an initial understanding of the problem, theoretical studies of the representativeness error have so far assumed that the covariance function of the unresolved scales is stationary and isotropic (Daley 1993; Mitchell and Daley 1997b; Desroziers et al. 2001; Liu and Rabier 2002). These assumptions lead conveniently to an expression for the representativeness error covariance matrix that depends on a small number of free parameters and that could potentially be implemented in operational practice. On the other hand, the creation

* Current affiliation: Alfred-Wegener Institute, Bremerhaven, Germany.

Corresponding author address: Tijana Janjić, Alfred-Wegener Institute, Bussestrasse 24, D-27570 Bremerhaven, Germany.
E-mail: t.janjic@iu-bremen.de

© 2006 American Meteorological Society

and destruction of unresolved scales is an effect of the local (in time and space) dynamics. Assumptions of stationarity and isotropy would therefore risk, if implemented in practice, underestimating the representativeness error variance when and where it is large, and overestimating it when and where it is small.

In the present study we consider data assimilation for the simple model problem of a passive tracer undergoing advection on the sphere. Shear in the advecting wind creates unresolved scales in the continuum state. The continuum state itself can be expressed in closed form for the idealized shear flow considered here, and in particular the resolved scales can be evolved exactly.[1] The observation operator is also known and discretized exactly. Therefore, the representativeness error is due solely to the unresolved scales. The continuum formalism of Cohn (1997) is used to develop and test two data assimilation schemes that treat this error. Both are extensions of the Kalman filter (Kalman 1960; Kalman and Bucy 1961) to continuum dynamics with discrete observations.

The first scheme is a version of the Schmidt–Kalman filter (Jazwinski 1970), which is essentially the generalized filter formulation of Mitchell and Daley (1997a,b). It accounts for state dependence and time correlation of the representativeness error but is not optimal. The second, simpler, scheme is a version of the traditional discrete Kalman filter, which does not account for these effects but does include a representativeness error covariance matrix. The numerical experiments show that both of these schemes work well for the model problem if they are supplied with the exact covariance function of the unresolved scales, which is neither stationary nor isotropic. The performance of the traditional filter is poor when it is instead given stationary, diagonal approximations of the representativeness error covariance matrix. Performance improves considerably when it is given a simple, time-dependent, but still diagonal approximation of the representativeness error covariance matrix.

The continuum formalism, specialized to the case of linear dynamics and observation operators, is reviewed in section 2. The data assimilation schemes are developed in section 3. The model problem and numerical experiments are described in section 4. Results are summarized in section 5.

2. The basic framework

We consider the problem of finding a finite-dimensional estimate of the state $w \equiv w(\mathbf{x}, t)$ of a continuum, linear, scalar dynamical system at given times t_k, using measurements available up to time t_k as well as our knowledge of the continuum system dynamics. Here, $\mathbf{x} \in \mathbb{R}^3$ denotes the space variables, w: $\mathbb{R}^4 \to \mathbb{R}$ lies in some function space $\mathcal{B}$, and we write

$$w(\mathbf{x}, t_k) = [F^c_{k,k-1} w_{k-1}](\mathbf{x}), \quad k = 1, 2, 3, \ldots, \tag{1}$$

where $F^c_{k,k-1}$:$\mathcal{B} \to \mathcal{B}$ is the solution operator from time t_{k-1} to time t_k for the partial differential equation that defines the continuum system dynamics. The solution operator acts on the function w at time t_{k-1}, and w_{k-1} denotes $w(\cdot, t_{k-1})$. We assume that the observations are linear functionals on the state, contaminated by additive noise:

$$\mathbf{w}^o_k = \mathbf{H}^c_k w(\cdot, t_k) + \boldsymbol{\epsilon}^m_k, \tag{2}$$

where $\mathbf{w}^o_k$ is the p_k vector of observations at time t_k, $\mathbf{H}^c_k$ is the *continuum forward observation operator* from $\mathcal{B}$ to $\mathbb{R}^{p_k}$, and $\boldsymbol{\epsilon}^m_k$ is the measurement error vector that depends on the instruments used to obtain the observations $\mathbf{w}^o_k$.

Applying the general formalism of Cohn (1997) to our scalar linear problem, we pose the finite-dimensional state estimation problem as that of estimating the projection

$$w^r(\mathbf{x}, t_k) \equiv [\Pi_k w_k](\mathbf{x}) \tag{3}$$

of the continuum state $w(\mathbf{x}, t_k)$ onto an N-dimensional subspace $\mathcal{B}^N_k$ of $\mathcal{B}$. Here, Π_k is a projection operator from $\mathcal{B}$ to $\mathcal{B}^N_k$, N is the dimension of the finite-dimensional state estimate that will be sought, and $w^r(\mathbf{x}, t_k)$ denotes the *resolved* portion of the continuum state. Denoting by $w^u(\mathbf{x}, t_k)$ the *unresolved* portion,

$$w^u(\mathbf{x}, t_k) \equiv [(I - \Pi_k) w_k](\mathbf{x}), \tag{4}$$

where I denotes the identity operator on $\mathcal{B}$, we have

$$w(\mathbf{x}, t_k) = w^r(\mathbf{x}, t_k) + w^u(\mathbf{x}, t_k). \tag{5}$$

The observation Eq. (2) can now be written in the form

$$\mathbf{w}^o_k = \mathbf{H}_k w^r(\cdot, t_k) + \boldsymbol{\epsilon}^o_k, \tag{6}$$

where $\mathbf{H}_k$ is the *discrete forward observation operator* from $\mathcal{B}^N_k$ to $\mathbb{R}^{p_k}$. The *observation error* $\boldsymbol{\epsilon}^o_k$ can be written as the sum of three parts:

$$\boldsymbol{\epsilon}^o_k = \boldsymbol{\epsilon}'_k + \boldsymbol{\epsilon}''_k + \boldsymbol{\epsilon}^m_k, \tag{7}$$

where

$$\boldsymbol{\epsilon}'_k \equiv \mathbf{H}^c_k w^u(\cdot, t_k), \tag{8}$$

[1] This is in contrast to the usual situation where there is "model error" due to unresolved scales, which has been studied recently by Hamill and Whitaker (2005).

will be called the *observation error due to unresolved scales*, and

$$\boldsymbol{\epsilon}_k'' \equiv [\mathbf{H}_k^c - \mathbf{H}_k]w^r(\cdot, t_k) \tag{9}$$

will be called the *forward interpolation error*.

According to (4), the observation error due to unresolved scales defined in (8) is the difference between a perfect (noise free) observation of the complete state w and a perfect observation of the resolved portion w^r, which we would like to have. It depends on all scales unresolved by elements of the finite-dimensional space $\mathcal{B}_k^N$. Accounting for this error in the estimation of w^r is the object of this study.

The forward interpolation error (9) contains the error caused by approximating the operator $\mathbf{H}_k^c$ with $\mathbf{H}_k$. This error is due to the particular discretization $\mathbf{H}_k$ chosen for $\mathbf{H}_k^c$, including any interpolation error due to representing the infinite-dimensional domain $\mathcal{B}$ of $\mathbf{H}_k^c$, with the finite-dimensional domain $\mathcal{B}_k^N$ of $\mathbf{H}_k$. To focus attention on the observation error due to unresolved scales, in this study we choose $\mathbf{H}_k$ to satisfy $[\mathbf{H}_k^c - \mathbf{H}_k]\Pi_k = 0$, that is, there is no forward interpolation error.

Note that our definitions of the terms in (7) are different from those used by some other authors. For example, the sum of the errors (8) and (9) is called the forward interpolation error by Daley (1993) and Mitchell and Daley (1997a,b). Also, this sum is called the representativeness error by Cohn (1997) and Lorenc (1986). The term "forward interpolation error" as defined in (9) is similar to the definition found in Daley (1991), except that our "true" state, that is, the state to be estimated, will be w^r rather than all of w. The term "representativeness error" is also used in Daley (1991) and Daley (1993) as the error due to the finite spacing L between observation locations; that is, it is defined there as "a measure of the error caused by the misrepresentation of all scales smaller than L."

Finally, from (1) we have

$$w^r(\mathbf{x}, t_k) = [F_{k,k-1}^r w_{k-1}^r](\mathbf{x}) + \delta'(\mathbf{x}, t_k) + \delta''(\mathbf{x}, t_k), \tag{10}$$

where $F_{k,k-1}^r : \mathcal{B}_{k-1}^N \to \mathcal{B}_k^N$ is the *discrete dynamical model*, or propagator, used to evolve the resolved scales;

$$\delta'(\mathbf{x}, t_k) \equiv [\Pi_k F_{k,k-1}^c w_{k-1}^u](\mathbf{x}) \tag{11}$$

is the *model error due to unresolved scales*; and

$$\delta''(\mathbf{x}, t_k) \equiv [(\Pi_k F_{k,k-1}^c - F_{k,k-1}^r) w_{k-1}^r](\mathbf{x}) \tag{12}$$

is the *model error due to discretization*. It is important to note that if $\mathcal{B}_k^N$ is defined in such a way that

$$\mathcal{B}_k^N \cap \mathrm{Range}[F_{k,k-1}^c(I - \Pi_{k-1})] = \emptyset, \tag{13}$$

where $\emptyset$ denotes the empty set, then there is no model error due to unresolved scales: $\delta'(\mathbf{x}, t_k) = 0$. We will choose $\mathcal{B}_k^N$ so that (13) holds, to isolate the observation error due to unresolved scales. Further, we will choose the discrete propagator $F_{k,k-1}^r$ to satisfy $[\Pi_k F_{k,k-1}^c - F_{k,k-1}^r]\Pi_{k-1} = 0$, so that there is no model error whatsoever and (10) becomes simply

$$w^r(\mathbf{x}, t_k) = [F_{k,k-1}^r w_{k-1}^r](\mathbf{x}). \tag{14}$$

From (1) it follows also that $w^u(\mathbf{x}, t_k)$ satisfies dynamics of the form

$$w^u(\mathbf{x}, t_k) = [F_{k,k-1}^u w_{k-1}^u](\mathbf{x}) + [F_{k,k-1}^{ur} w_{k-1}^r](\mathbf{x}), \tag{15}$$

where $F_{k,k-1}^u$ and $F_{k,k-1}^{ur}$ represent the action of $(I - \Pi_k)F_{k,k-1}^c$ on $\mathcal{B}\backslash\mathcal{B}_k^N$ and $\mathcal{B}_k^N$, respectively. The second term on the right-hand side of (15) vanishes in case

$$\mathcal{B}\backslash\mathcal{B}_k^N \cap \mathrm{Range}(F_{k,k-1}^c \Pi_{k-1}) = \emptyset, \tag{16}$$

in which case the dynamics of the resolved and unresolved scales are fully decoupled in view of (14). We do not assume (16); that is, while we choose $\mathcal{B}_k^N$ so that the unresolved scales do not influence the resolved scales, we allow the resolved scales to influence the unresolved ones. In any case, (15) is an infinite-dimensional equation and cannot be evolved exactly in general.

3. The state estimation problem

The objective is now to estimate the state $w^r(\mathbf{x}, t_k)$ using measurements

$$\mathbf{w}_k^o = \mathbf{H}_k w^r(\cdot, t_k) + \boldsymbol{\epsilon}_k^o, \tag{17}$$

where the observation error $\boldsymbol{\epsilon}_k^o$ is

$$\boldsymbol{\epsilon}_k^o = \mathbf{H}_k^c w^u(\cdot, t_k) + \boldsymbol{\epsilon}_k^m; \tag{18}$$

the state w^r evolves according to (14) with random initial condition $w^r(\mathbf{x}, t_0)$, and w^u evolves according to (15) with random initial condition $w^u(\mathbf{x}, t_0)$. The measurement error $\boldsymbol{\epsilon}_k^m$ is assumed to be normally distributed with mean zero and covariance matrix $\mathbf{R}_k$, that is, $\boldsymbol{\epsilon}_k^m \sim \mathcal{N}(0, \mathbf{R}_k)$, and to be white in time, and uncorrelated with $w^r(\mathbf{x}, t)$ and $w^u(\mathbf{x}, t)$ at all times. Note that (18) and (15) imply that $\boldsymbol{\epsilon}_k^o$ is sequentially correlated and is also correlated with the state w^r. Also, (18) and (15) imply that the mean of $\boldsymbol{\epsilon}_k^o$ is not necessarily zero, even if we

assume that $\langle w^u(\mathbf{x}, t_0)\rangle = 0$, due to the possible contribution from resolved scales to $\langle w^u(\mathbf{x}, t_k)\rangle$. Here, $\langle\cdot\rangle$ denotes the mathematical expectation.

Having introduced the basic definitions and assumptions, we turn our attention to methods for estimating $w^r(\mathbf{x}, t)$. Three different approaches will be considered.

a. The Kalman filter

Since $\boldsymbol{\epsilon}_k^o$ is sequentially correlated and correlated with the state w^r, the usual Kalman filter equations cannot be applied directly to the system (14) and (17). However, one can write the augmented system:

$$\begin{bmatrix} w^r(\mathbf{x}, t_k) \\ w^u(\mathbf{x}, t_k) \end{bmatrix} = \begin{bmatrix} F^r_{k,k-1} & 0 \\ F^{ur}_{k,k-1} & F^u_{k,k-1} \end{bmatrix} \begin{bmatrix} w^r_{k-1} \\ w^u_{k-1} \end{bmatrix}(\mathbf{x}), \tag{19}$$

with the observations given by

$$\mathbf{w}_k^o = [\mathbf{H}_k\ \mathbf{H}_k^c] \begin{bmatrix} w^r(\cdot, t_k) \\ w^u(\cdot, t_k) \end{bmatrix} + \boldsymbol{\epsilon}_k^m. \tag{20}$$

For the augmented system, the observation error $\boldsymbol{\epsilon}_k^m$ has mean zero and is neither sequentially correlated nor correlated with the augmented state vector that must now be estimated, and the Kalman filter equations apply. However, with this approach, w^u is estimated simultaneously with w^r and the evolution of the error covariance function of the unresolved scales and of the error cross-covariance function between the resolved and unresolved scales is required. This makes the full Kalman filter approach unsuitable, since these are functions that belong to an infinite-dimensional space and cannot be computed in practice. Although we have accounted for the observation error due to unresolved scales, some approximation is needed.

b. The Schmidt–Kalman filter

The second approach discussed here is similar to the Schmidt–Kalman formulation (Jazwinski 1970). The Schmidt–Kalman filter equations can be obtained by first writing the standard Kalman filter for the augmented system (19) and (20), and then neglecting terms containing estimates of w^u. This leads to the analysis update

$$w_k^{r,a}(\mathbf{x}) = w_k^{r,f}(\mathbf{x}) + \mathbf{K}_k^r(\mathbf{x})[\mathbf{w}_k^o - \mathbf{H}_k w_k^{r,f}(\cdot) - \mathbf{H}_k^c\langle w^u(\cdot, t_k)\rangle], \tag{21}$$

$$\mathbf{K}_k^r(\mathbf{x}) = [\mathbf{H}_k S_k^{rr,f}(\mathbf{x}, \cdot) + \mathbf{H}_k^c S_k^{ru,f}(\mathbf{x}, \cdot)]^{\mathrm{T}} \mathbf{M}_k^{-1}, \tag{22}$$

$$S_k^{rr,a}(\mathbf{x}_1, \mathbf{x}_2) = S_k^{rr,f}(\mathbf{x}_1, \mathbf{x}_2) - \mathbf{K}_k^r(\mathbf{x}_1)[\mathbf{H}_k S_k^{rr,f}(\cdot, \mathbf{x}_2) + \mathbf{H}_k^c S_k^{ru,f}(\mathbf{x}_2, \cdot)], \tag{23}$$

$$S_k^{ru,a}(\mathbf{x}_1, \mathbf{x}_2) = S_k^{ru,f}(\mathbf{x}_1, \mathbf{x}_2) - \mathbf{K}_k^r(\mathbf{x}_1)[\mathbf{H}_k^c C_k^u(\cdot, \mathbf{x}_2) + \mathbf{H}_k S_k^{ru,f}(\cdot, \mathbf{x}_2)], \tag{24}$$

$$\mathbf{M}_k = \mathbf{H}_{2k}[\mathbf{H}_{1k} S_k^{rr,f}(\cdot, \cdot)]^{\mathrm{T}} + \mathbf{H}_{2k}^c[\mathbf{H}_{1k} S_k^{ru,f}(\cdot, \cdot)]^{\mathrm{T}} + \mathbf{H}_{1k}[\mathbf{H}_{2k}^c S_k^{ru,f}(\cdot, \cdot)]^{\mathrm{T}} + \mathbf{H}_{2k}^c[\mathbf{H}_{1k}^c C_k^u(\cdot, \cdot)]^{\mathrm{T}} + \mathbf{R}_k, \tag{25}$$

and the forecast equations

$$w_k^{r,f}(\mathbf{x}) = [F^r_{k,k-1} w^{r,a}_{k-1}](\mathbf{x}), \tag{26}$$

$$S_k^{rr,f}(\mathbf{x}_1, \mathbf{x}_2) = [F^r_{2k,k-1} F^r_{1k,k-1} S^{rr,a}_{k-1}](\mathbf{x}_1, \mathbf{x}_2), \quad \text{and} \tag{27}$$

$$S_k^{ru,f}(\mathbf{x}_1, \mathbf{x}_2) = [F^u_{2k,k-1} F^r_{1k,k-1} S^{ru,a}_{k-1}](\mathbf{x}_1, \mathbf{x}_2) + [F^{ur}_{2k,k-1} F^r_{1k,k-1} S^{rr,a}_{k-1}](\mathbf{x}_1, \mathbf{x}_2). \tag{28}$$

The operators $\mathbf{H}_{1k}$ and $\mathbf{H}_{1k}^c$ in (25) act on the $\mathbf{x}_1$ variables, while $\mathbf{H}_{2k}$ and $\mathbf{H}_{2k}^c$ act on the $\mathbf{x}_2$ variables. Thus, $\mathbf{H}_{1k}^c C_k^u(\cdot, \mathbf{x}_2)$ is a (column-) vector-valued function of $\mathbf{x}_2$, for instance, and $\mathbf{H}_{2k}^c[\mathbf{H}_{1k}^c C_k^u(\cdot, \cdot)]^{\mathrm{T}}$ is a $p_k \times p_k$ matrix. Operators such as $F^r_{1k,k-1}$ and $F^r_{2k,k-1}$ in (27) are defined similarly.

The covariance function $C_k^u(\mathbf{x}_1, \mathbf{x}_2)$ in (24) and (25) is supposed to approximate the covariance function of the unresolved scales defined by

$$W^{uu}(\mathbf{x}_1, \mathbf{x}_2, t_k) \equiv \langle [w^u(\mathbf{x}_1, t_k) - \langle w^u(\mathbf{x}_1, t_k)\rangle] \times [w^u(\mathbf{x}_2, t_k) - \langle w^u(\mathbf{x}_2, t_k)\rangle]\rangle. \tag{29}$$

The usual Schmidt–Kalman formulation takes $C_k^u(\mathbf{x}_1, \mathbf{x}_2) = W^{uu}(\mathbf{x}_1, \mathbf{x}_2, t_0)$, but we consider $C_k^u(\mathbf{x}_1, \mathbf{x}_2)$ to model $W^{uu}(\mathbf{x}_1, \mathbf{x}_2, t_k)$, and, therefore, to depend on time in general. Still, this filter is suboptimal since w^u is not estimated. The covariances calculated by Eqs. (23), (24), (27), and (28) are also not the estimation error covariances. The actual estimation error covariances are defined by

$$P_k^{rr,f}(\mathbf{x}_1, \mathbf{x}_2) \equiv \langle [w^r(\mathbf{x}_1, t_k) - w_k^{r,f}(\mathbf{x}_1)] \times [w^r(\mathbf{x}_2, t_k) - w_k^{r,f}(\mathbf{x}_2)]\rangle, \tag{30}$$

and similarly for $P_k^{rr,a}$. Recursions for the actual estimation error covariances are derived in Janjić (2001).

If the unresolved-scales covariance function $W^{uu}(\mathbf{x}_1, \mathbf{x}_2, t_k)$ were actually known, then $C_k^u(\mathbf{x}_1, \mathbf{x}_2)$ could be set equal to $W^{uu}(\mathbf{x}_1, \mathbf{x}_2, t_k)$. In this case, it can be seen that Eqs. (21)–(28), with an assumption that the mean of the unresolved scales is zero, are essentially identical to the formulas given in Mitchell and Daley (1997a,b), which were obtained in a discrete setting by searching for the gain that minimizes the trace of the matrix obtained by evaluating $S_k^{rr,a}(\mathbf{x}_1, \mathbf{x}_2)$ at grid points. Also, in this spe-

cial case it can be shown that the computed covariances $S_k^{rr,f}$ and $S_k^{rr,a}$ are the same as the actual estimation error covariances $P_k^{rr,f}$ and $P_k^{rr,a}$ (see Jazwinski 1970, Example 8.2).

c. The traditional filter

The third formulation can be derived from the Schmidt–Kalman filter equations by setting $S_k^{ru,f}$ and $S_k^{ru,a}$ to zero. It can also be derived by assuming that $\boldsymbol{\epsilon}_k^o \sim \mathcal{N}(0, \mathbf{H}_{2k}^c[\mathbf{H}_{1k}^c C_k^u(\cdot,\cdot)]^{\mathrm{T}} + \mathbf{R}_k)$ with $\mathbf{H}_{2k}^c[\mathbf{H}_{1k}^c C_k^u(\cdot,\cdot)]^{\mathrm{T}}$ given a priori, and neglecting the sequential correlation of the observation error defined in (18) (see Cohn 1997) and the correlation between the observation error and the state w^r. With this approach, the estimation equations are

$$w_k^{r,a}(\mathbf{x}) = w_k^{r,f}(\mathbf{x}) + \mathbf{K}_k^r(\mathbf{x})[(\mathbf{w}_k^o - \mathbf{H}_k w_k^{r,f}(\cdot) - \mathbf{H}_k^c\langle w^u(\cdot, t_k)\rangle], \tag{31}$$

$$\mathbf{K}_k^r(\mathbf{x}) = [\mathbf{H}_k S_k^{rr,f}(\mathbf{x},\cdot)]^{\mathrm{T}}\mathbf{M}_k^{-1}, \tag{32}$$

$$S_k^{rr,a}(\mathbf{x}_1,\mathbf{x}_2) = S_k^{rr,f}(\mathbf{x}_1,\mathbf{x}_2) - \mathbf{K}_k^r(\mathbf{x}_1)\mathbf{H}_k S_k^{rr,f}(\cdot,\mathbf{x}_2), \tag{33}$$

and

$$\mathbf{M}_k = \mathbf{H}_{2k}[\mathbf{H}_{1k} S_k^{rr,f}(\cdot,\cdot)]^{\mathrm{T}} + \mathbf{H}_{2k}^c[\mathbf{H}_{1k}^c C_k^u(\cdot,\cdot)]^{\mathrm{T}} + \mathbf{R}_k, \tag{34}$$

along with (26) and (27). This filter can be implemented exactly, because all the equations are for functions in the finite-dimensional subspace $\mathcal{B}_k^N$. Also, for application of this filter, $\mathbf{H}_{2k}^c[\mathbf{H}_{1k}^c C_k^u(\cdot,\cdot)]^{\mathrm{T}}$ is needed, in contrast to the full $C_k^u(\mathbf{x}_1, \mathbf{x}_2)$ needed for the Schmidt–Kalman approach. Recursions for the actual estimation error covariances arising from this filter are derived in Janjić (2001).

Suppose now that $\mathcal{B}$ is a Hilbert space. Then, $\mathcal{B}_k^N$ is best viewed as a finite-dimensional Hilbert space, and w^r can be expanded in terms of orthogonal basis functions $\mu_{i,k}(\mathbf{x})$, $i = 1, \ldots N$, of $\mathcal{B}_k^N$. We denote the $N \times 1$ vector of expansion coefficients for w^r as $\hat{\mathbf{w}}^{\mathbf{r}}$, the $N \times N$ matrices of expansion coefficients of the functions $S_k^{rr,f}$, $S_k^{rr,a}$ as $\hat{\mathbf{S}}_k^{rr,f}$, $\hat{\mathbf{S}}_k^{rr,a}$, and the $N \times p_k$ matrix of expansion coefficients of the p_k-row vector $\mathbf{K}_k^r(\mathbf{x})$ as $\hat{\mathbf{K}}_k^r$. Also, we define $\hat{\mathbf{F}}_{k,k-1}^r$ as the $N \times N$ matrix whose elements are

$$[\hat{\mathbf{F}}_{k,k-1}^r]_{ij} \equiv \int \mu_{i,k}(\mathbf{x})\,[F_{k,k-1}^r \mu_{j,k-1}](\mathbf{x}, t_k)\,d\mathbf{x}, \tag{35}$$

and $\hat{\mathbf{H}}_k$ as the $p_k \times N$ matrix given by

$$\hat{\mathbf{H}}_k \equiv [\mathbf{H}_k\mu_{1,k}(\cdot), \ldots, \mathbf{H}_k\mu_{N,k}(\cdot)]. \tag{36}$$

Using this notation the traditional filter Eqs. (31)–(34), (26), and (27) become

$$\hat{\mathbf{w}}_k^{r,a} = \hat{\mathbf{w}}_k^{r,f} + \hat{\mathbf{K}}_k^r(\mathbf{w}_k^o - \hat{\mathbf{H}}_k\hat{\mathbf{w}}_k^{r,f} - \mathbf{H}_k^c\langle w^u(\cdot, t_k)\rangle), \tag{37}$$

$$\hat{\mathbf{K}}_k^r = \hat{\mathbf{S}}_k^{rr,f}\hat{\mathbf{H}}_k^{\mathrm{T}}\mathbf{M}_k^{-1}, \tag{38}$$

$$\hat{\mathbf{S}}_k^{rr,a} = \hat{\mathbf{S}}_k^{rr,f} - \hat{\mathbf{K}}_k^r\hat{\mathbf{H}}_k\hat{\mathbf{S}}_k^{rr,f}, \tag{39}$$

$$\mathbf{M}_k = \hat{\mathbf{H}}_k\hat{\mathbf{S}}_k^{rr,f}\hat{\mathbf{H}}_k^{\mathrm{T}} + \mathbf{H}_{2k}^c[\mathbf{H}_{1k}^c C_k^u(\cdot,\cdot)]^{\mathrm{T}} + \mathbf{R}_k, \tag{40}$$

and

$$\hat{\mathbf{w}}_k^{r,f} = \hat{\mathbf{F}}_{k,k-1}^r\hat{\mathbf{w}}_{k-1}^{r,a}, \tag{41}$$

$$\hat{\mathbf{S}}_k^{rr,f} = \hat{\mathbf{F}}_{k,k-1}^r\hat{\mathbf{S}}_{k-1}^{rr,a}(\hat{\mathbf{F}}_{k,k-1}^r)^{\mathrm{T}}. \tag{42}$$

Equations (37)–(42) have the form of a discrete Kalman filter but include a representativeness (unresolved scales) mean in (37) and a representativeness (unresolved scales) error covariance term in (40) because they have been derived from first principles from the continuum Kalman filter.

4. An example for advective dynamics

In this section, an analytical example is formulated in order to test the assimilation methods introduced in section 3. For this example we demonstrate first that the traditional filter and the Schmidt–Kalman filter both work well given the exact covariance function W^{uu}. However, since this requirement cannot be satisfied in practice, the traditional filter is then tested under more realistic conditions, using a conventional model for the covariance matrix $\mathbf{H}_{2k}^c[\mathbf{H}_{1k}^c C_k^u(\cdot,\cdot)]^{\mathrm{T}}$. After describing tests with the conventional model, which failed to give satisfactory results, a more successful model is then formulated and tested.

a. Model dynamics

An analytical solution describing advection dynamics on the sphere is needed to avoid introducing numerical modeling errors into the assimilation procedure. In this way, only initial error, measurement error, and the observation error due to unresolved scales will be present in the estimation problem. However, in order to test properly the assimilation methods discussed in section 3, the analytical solution must depict a sufficiently complex dynamical process. Few such analytical solutions on the sphere are available (e.g., Williamson et al. 1992), and none that we know of is adequate for our study (Janjić 2001). For this reason an appropriate model dynamics is defined here, and the corresponding solution is found and examined.

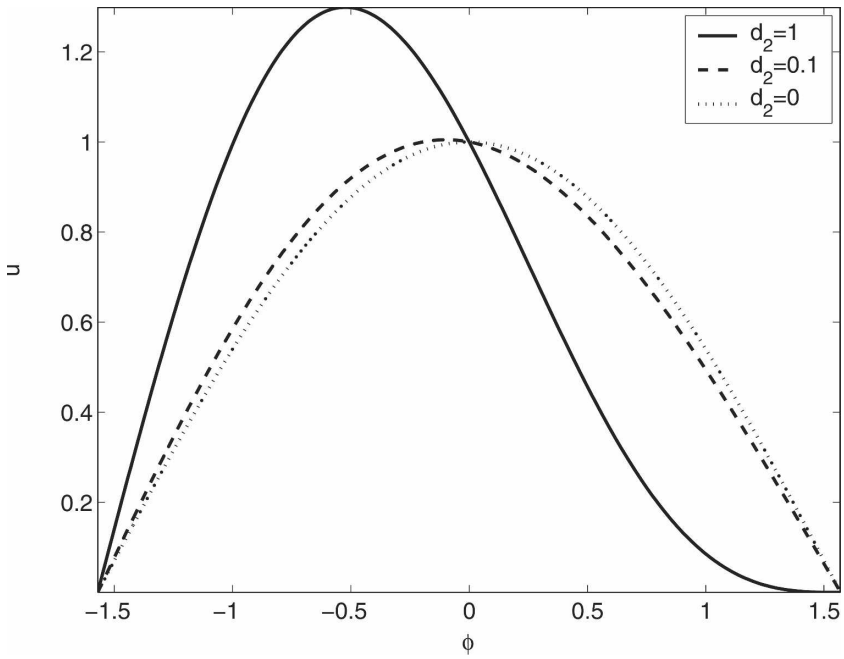

FIG. 1. Zonal velocity (in dimensionless units; see text) for $d_2 = 1$ (solid line), $d_2 = 0.1$ (dashed line), and $d_2 = 0$ (dotted line), as a function of latitude ϕ in radians.

Consider the two-dimensional advection equation on the sphere with nondivergent advecting wind,

$$\frac{\partial w}{\partial t} - \frac{1}{a^2 \cos\varphi}\frac{\partial \Psi}{\partial \varphi}\frac{\partial w}{\partial \lambda} + \frac{1}{a^2 \cos\varphi}\frac{\partial \Psi}{\partial \lambda}\frac{\partial w}{\partial \varphi} = 0, \quad (43)$$

$$w(\lambda, \varphi, 0) = w_0(\lambda, \varphi), \quad (44)$$

where a is the radius of the sphere, $\lambda \in [0, 2\pi]$ is longitude, $\varphi \in [-\pi/2, \pi/2]$ is latitude, Ψ is the streamfunction, and $t \in [0, \infty)$ is time. We take $\Psi = \Psi(\lambda, \varphi)$ to be independent of time. The solution $w(\lambda, \varphi, t)$ of (43) is sought for arbitrary initial condition (44).

We consider streamfunctions of the form

$$\Psi(\lambda, \varphi) = d_1 a^2 \sin\varphi + \frac{d_2 a^2}{6}(3\sin^2\varphi - 1), \quad (45)$$

with $d_1 = -1$. The corresponding velocity vector has zonal and meridional velocity components, respectively,

$$u = -d_1 a \cos\varphi - d_2 a \cos\varphi \sin\varphi, \quad \upsilon = 0. \quad (46)$$

Here, a is chosen as the unit for measuring distance, so that at $\varphi = 0$ the distance an air parcel travels over a time interval of length 1 is a. For a typical atmospheric advection speed on the order of 20 m s^{-1}, the time scale $t = 2\pi$ corresponds to a little more than 23 days. Profiles of u are shown in Fig. 1 for $d_2 = 1$ (solid line), $d_2 = 0.1$ (dashed line), and $d_2 = 0$ (dotted line). Note that for $d_2 = 0$, we have solid-body rotation. Nonzero d_2 introduces shear into the flow, which creates anisotropy of the estimation error covariance (Ménard et al. 2000). It also introduces unresolved scales.

In our case of the streamfunction depending only on φ, the solution of the advection Eqs. (43) and (44) can be obtained readily by the method of characteristics. For the streamfunction (45), the general solution is

$$w(\lambda, \varphi, t) = w_0(\lambda + d_1 t + d_2 t \sin\varphi, \varphi). \quad (47)$$

In particular, the solution for the initial condition given by

$$w(\lambda, \varphi, 0) = a_1 \sin\varphi + a_2 \cos\lambda \cos\varphi + a_3 \sin\lambda \cos\varphi \quad (48)$$

is

$$w(\lambda, \varphi, t) = a_1 \sin\varphi + a_2 \cos(\lambda + d_1 t + d_2 t \sin\varphi)\cos\varphi + a_3 \sin(\lambda + d_1 t + d_2 t \sin\varphi)\cos\varphi. \quad (49)$$

Solutions of (43) and (44) for more general streamfunctions, depending on λ as well as φ, are given in Janjić (2001).

The initial condition (48) can be written in terms of the spherical harmonics as

$$w(\lambda, \varphi, 0) = \hat{w}_{10}(0) Y_1^0(\lambda, \varphi) + \hat{w}_{11}(0) Y_1^1(\lambda, \varphi) + \hat{w}_{1,-1}(0) Y_1^{-1}(\lambda, \varphi), \quad (50)$$

with

$$\hat{w}_{10}(0) = \frac{a_1}{A_{10}}, \quad \hat{w}_{11}(0) = \frac{a_2}{2A_{11}} - \frac{ia_3}{2A_{11}},$$
$$\hat{w}_{1,-1}(0) = -\overline{\hat{w}_{1,1}(0)}. \tag{51}$$

Here, we denote by $Y_l^m(\lambda, \varphi)$ the spherical harmonic (e.g., Arfken 1995):

$$Y_l^m(\lambda, \varphi) = A_{lm} P_l^{|m|}(\sin\varphi) e^{im\lambda}, \tag{52}$$

where $P_l^{|m|}$ is the associated Legendre function and

$$A_{lm} = \left[\frac{2l+1}{4\pi}\frac{(l-|m|)!}{(l+|m|)!}\right]^{(1/2)} \times \begin{cases} (-1)^m & \text{if} \quad m \geq 0 \\ 1 & \text{if} \quad m < 0 \end{cases}. \tag{53}$$

The corresponding solution (49) of the advection equation can be expanded in terms of the spherical harmonics as

$$w(\lambda, \varphi, t) = \sum_{l=0}^{\infty} \sum_{m=-l}^{l} \hat{w}_{lm}(t) Y_l^m(\lambda, \varphi), \tag{54}$$

with

$$\hat{w}_{l0}(t) = \hat{w}_{l0}(0), \quad \text{for} \quad l \geq 0,$$
$$\hat{w}_{l1}(t) = \hat{w}_{11}(0) e^{id_1 t} \frac{A_{11}}{A_{l1}} i^{(l-1)}[j_{l-1}(d_2 t) + j_{l+1}(d_2 t)], \quad \text{for} \quad l \geq 1,$$
$$\hat{w}_{l,-1}(t) = -\overline{\hat{w}_{l1}(t)}, \quad \text{for} \quad l \geq 1,$$
$$\hat{w}_{lm}(t) = 0, \quad \text{for} \quad l \geq |m| \geq 2, \tag{55}$$

where j_i for $i = 0, 1, \ldots,$ are the spherical Bessel functions (see appendix A). Although only three spherical harmonics are present at the initial time, infinitely many harmonics are generated for $t > 0$ in general, due to the shear flow for $d_2 \neq 0$. In the solid-body rotation case $d_2 = 0$, the number of nonzero spherical harmonic coefficients remains the same as in the initial condition.

We consider only nonzero values of d_2 in the experiments, and therefore nonzero coefficients of the spherical harmonics are always generated. The numerical value of the coefficient d_2 determines how quickly the spherical harmonic spectrum of the solution evolves. Thus, the success of state estimation procedures can be expected to depend on the value of d_2.

b. State estimation

The state to be estimated is taken to be a truncated version of the expansion (54); namely,

$$w^r(\lambda, \varphi, t) = \sum_{l=0}^{1} \sum_{m=-l}^{l} \hat{w}_{lm}(t) Y_l^m(\lambda, \varphi), \tag{56}$$

where $\hat{w}_{lm}(t)$ are defined by (55). For the initial condition (48), we take the coefficients $a_i \sim \mathcal{N}(0, 1)$ to be uncorrelated with each other, or $\langle a_i a_j \rangle = 0$ for $i \neq j$.

Equation (56) serves to define the resolved subspace $\mathcal{B}_k^N$ for our example: it consists of all linear combinations of the spherical harmonics Y_1^0, Y_1^{-1} and Y_1^1. Thus, $\mathcal{B}_k^N$ is independent of time t_k and has dimension $N = 3$. It can be verified that (13) is satisfied while (16) is not. Equation (56) also defines the projection operator Π_k: it is the identity operator on $\mathcal{B}_k^N$, and the zero operator on $\mathcal{B} \backslash \mathcal{B}_k^N$.

We point out that a discretization is possible that ensures that both (13) and (16) are satisfied. Namely, in the case of fully Lagrangian discretization with the resolved scales defined as volume averages over N Lagrangian trajectories, the resolved and unresolved scales are dynamically decoupled and evolve separately (Lyster et al. 2004). While the Lagrangian approach has many practical advantages, the spherical harmonic discretization is better suited to the detailed investigation described here.

The state estimation is carried out with initial condition $w_0^{r,a}(\lambda, \varphi) = 0$, and since $\langle w_0^r(\lambda, \varphi) \rangle = 0$, the initial covariance functions are given by

$$S_0^{rr,a}(\lambda_1, \varphi_1, \lambda_2, \varphi_2) = \langle w_0(\lambda_1, \varphi_1) w_0(\lambda_2, \varphi_2) \rangle,$$
$$S_0^{ru,a}(\lambda_1, \varphi_1, \lambda_2, \varphi_2) = 0. \tag{57}$$

Note that the initial covariance function $S_0^{rr,a}$ is isotropic, since from (48) we have that

$$\begin{aligned} \langle w_0(\lambda_1, \varphi_1) w_0(\lambda_2, \varphi_2) \rangle &= \langle a_1^2 \rangle \sin\varphi_1 \sin\varphi_2 \\ &\quad + \langle a_2^2 \rangle \cos\lambda_1 \cos\lambda_2 \cos\varphi_1 \cos\varphi_2 \\ &\quad + \langle a_3^2 \rangle \sin\lambda_1 \sin\lambda_2 \cos\varphi_1 \cos\varphi_2 \\ &= \cos\gamma, \end{aligned} \tag{58}$$

where γ is the spherical angle subtended by the points (λ_1, φ_1) and (λ_2, φ_2); compare with Gaspari and Cohn (1999, Example 2.6). Also, by (49) and our assumptions on the a_i, it follows that $\langle w(\lambda, \varphi, t) \rangle = 0$ for all t, and from (51) and (55) it follows that $\langle w^r(\lambda, \varphi, t) \rangle = 0$ also. Therefore, in our experiments $\langle w^u(\lambda, \varphi, t) \rangle = 0$ for all times t.

The observations are taken as the values of the analytical solution (49) at the observation points, with a small normally distributed measurement error $\boldsymbol{\epsilon}_k^m \sim \mathcal{N}(0, 10^{-6}\mathbf{I})$. Therefore, as can be seen from (55), the observations contain all scales of motion. Taking point observations is justified because the full state (49) is

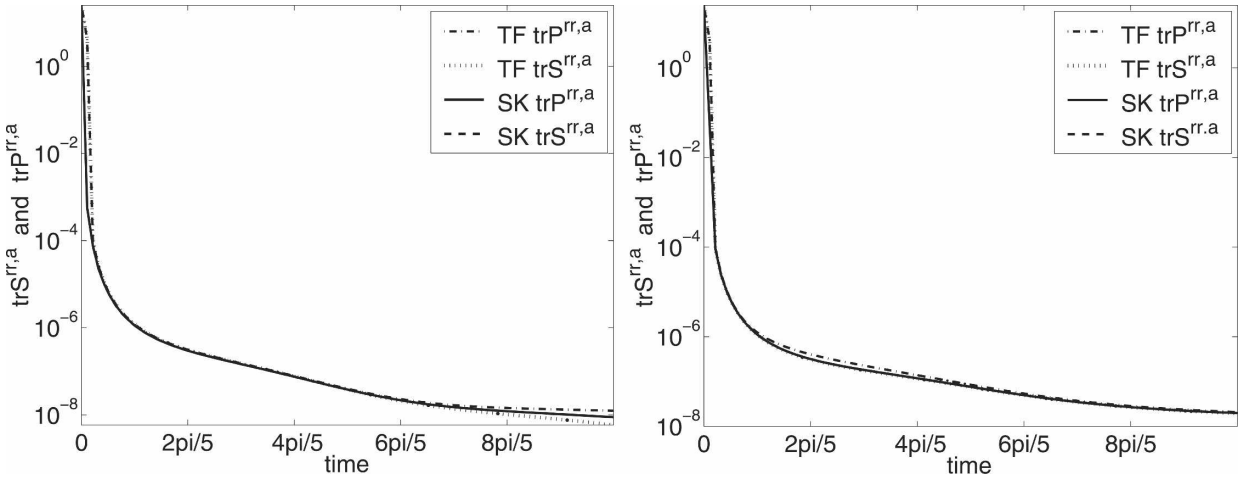

FIG. 2. Comparison of the actual and computed covariances for the Schmidt–Kalman filter and the traditional filter, for both (left) $d_2 = 1$ and (right) $d_2 = 0.1$. The trace of the computed covariance $S_k^{rr,a}$ of the traditional filter is denoted by the dotted line, and that of the actual covariance $P_k^{rr,a}$ for the traditional filter by the dashed–dotted line. The trace of the computed covariance of the Schmidt–Kalman filter is denoted by the dashed line, and that of the actual covariance for the Schmidt–Kalman filter coincides with the computed one, and is denoted by the solid line. Log scale is used on the ordinate, where the units are arbitrary. The abscissa is time in dimensionless units as described in the text.

bounded and continuous for all finite time. The observations are taken to be located at 41 equally spaced points along the meridian $\lambda = \pi$. The assimilation is carried out at 92 instants per time cycle of length 2π. This corresponds to assimilation approximately every 6 h during 23 days.

c. *Experiments with the exact unresolved-scales covariance function*

The first tests are done using the traditional filter and the Schmidt–Kalman filter, and taking $C_k^u(\mathbf{x}_1, \mathbf{x}_2) = W^{uu}(\mathbf{x}_1, \mathbf{x}_2, t_k)$ since W^{uu} defined in (29) is known exactly in our model problem. It is calculated analytically, using the formula

$$\begin{aligned} W^{uu}(\lambda_1, \varphi_1, \lambda_2, \varphi_2, t) = {} & W(\lambda_1, \varphi_1, \lambda_2, \varphi_2, t) \\ & + W^{rr}(\lambda_1, \varphi_1, \lambda_2, \varphi_2, t) \\ & - \langle w(\lambda_1, \varphi_1, t) w^r(\lambda_2, \varphi_2, t)\rangle \\ & - \langle w^r(\lambda_1, \varphi_1, t) w(\lambda_2, \varphi_2, t)\rangle, \end{aligned} \tag{59}$$

where

$$\begin{aligned} W(\mathbf{x}_1, \mathbf{x}_2, t_k) &\equiv \langle w(\mathbf{x}_1, t_k) w(\mathbf{x}_2, t_k)\rangle, W^{rr}(\mathbf{x}_1, \mathbf{x}_2, t_k) \\ &\equiv \langle w^r(\mathbf{x}_1, t_k) w^r(\mathbf{x}_2, t_k)\rangle. \end{aligned} \tag{60}$$

In (59), W is calculated by the method of characteristics from the initial covariance given in (58). The resolved-scales covariance function W^{rr} is calculated using (51), (55), and the assumptions on the coefficients a_i stated after (56). The cross-covariance function $\langle w(\lambda_1, \varphi_1, t) w^r(\lambda_2, \varphi_2, t)\rangle$ is calculated using (49), (55), and (56).

Both methods performed well for both values of d_2 tested. This can be seen from Fig. 2, which shows for $d_2 = 1$ (left panel) and $d_2 = 0.1$ (right panel) the trace of the computed and actual covariance functions defined by the formulas

$$\mathrm{tr} S_k^{rr,a} \equiv \int_0^{2\pi} \int_{-\pi/2}^{\pi/2} S_k^{rr,a}(\lambda, \varphi, \lambda, \varphi) \cos\varphi \, d\lambda \, d\varphi, \tag{61}$$

$$\mathrm{tr} P_k^{rr,a} \equiv \int_0^{2\pi} \int_{-\pi/2}^{\pi/2} P_k^{rr,a}(\lambda, \varphi, \lambda, \varphi) \cos\varphi \, d\lambda \, d\varphi. \tag{62}$$

These integrals are calculated analytically for our model problem. The results shown in Fig. 2 suggest that the time correlation of the observation error, and its correlation with the state, which are ignored by the traditional filter, in this example do not have a significant deleterious impact on the assimilation.

However, to use the traditional filter in practice, an estimate of the unresolved-scales covariance matrix $\mathbf{H}_{2k}^c[\mathbf{H}_{1k}^c W^{uu}(\cdot, \cdot, t_k)]^{\mathrm{T}}$ at the observation locations is needed. Rather than use our knowledge of this covariance, in subsequent experiments we model it by $\mathbf{H}_{2k}^c[\mathbf{H}_{1k}^c C_k^u(\cdot, \cdot)]^{\mathrm{T}}$. We note that initially $W^{uu}(\lambda_1, \varphi_1, \lambda_2, \varphi_2, 0) = 0$, since $w^u(\lambda, \varphi, 0) = 0$ for all λ, φ. Also $W^{uu}(\lambda_1,$

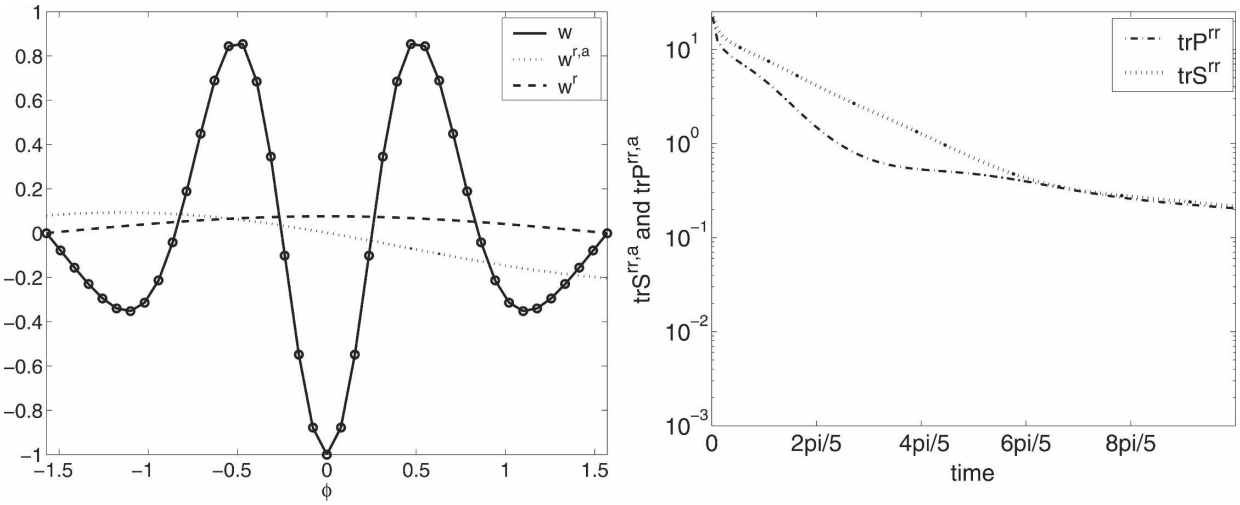

FIG. 3. (left) Cross section at $\lambda = \pi$ of the state estimate $w^{r,a}(\lambda, \varphi, t)$ (dotted line), the state $w^r(\lambda, \varphi, t)$ (dashed line), the full state $w(\lambda, \varphi, t)$ (solid line), and the observations (circles) for $d_2 = 1$, at $t = 2\pi$, obtained with the traditional filter and $\mathbf{H}^c_{2k}[\mathbf{H}^c_{1k}W^{uu}(\cdot, \cdot, t_k)]^{\mathrm{T}}$ approximated by $31\mathbf{I}$, and (right) comparison in time of the trace of the actual (dashed–dotted line) and computed (dotted line) covariances, $P^{rr,a}_k$ and $S^{rr,a}_k$, respectively, for this traditional filter. The realization of the initial conditions used for the left panel is $a_1 = 0$, $a_2 = 1$, and $a_3 = 0$, where units on the ordinate are arbitrary and the abscissa is the latitude ϕ in radians. Log scale in arbitrary units is used on the ordinate in the right panel, where the abscissa is time in dimensionless units.

$\varphi_1, \lambda_2, \varphi_2, t)$ is not isotropic for all $t > 0$ (see Janjić 2001). However, $W^{uu}(\lambda_1, \varphi_1, \lambda_2, \varphi_2, t)$ does depend on λ_1 and λ_2 only through dependence on $\lambda_1 - \lambda_2$, at all times t. The matrix $\mathbf{H}^c_{2k}[\mathbf{H}^c_{1k}W^{uu}(\cdot, \cdot, t_k)]^{\mathrm{T}}$ is not close to a diagonal matrix. For instance, the ratio of the sum of the diagonal elements to the sum of the absolute values of all the elements of this matrix is maximal for $d_2 = 1$ at approximately $t = 6.5\pi$ and is about 0.05 (result not shown), whereas a value of 1.0 would be obtained for a diagonal matrix.

d. Experiments using a modeled covariance

A simple approximation is to take the unresolved-scales covariance matrix at observation locations to be diagonal and constant in time: $\mathbf{H}^c_{2k}[\mathbf{H}^c_{1k}C^u_k(\cdot, \cdot)]^{\mathrm{T}} = \sigma^2\mathbf{I}$. This approximation mimics the operational practice of accounting for the observation error due to unresolved scales by increasing the diagonal of the measurement error covariance matrix $\mathbf{R}$ by some fixed amount (e.g., Courtier et al. 1998, their appendix B). It does not generally give satisfactory results for the traditional filter in our model problem, as can be seen in Figs. 3 and 4. In the left panels of Figs. 3 and 4 are the cross sections of the fields $w^r(\lambda, \varphi, 2\pi)$, $w(\lambda, \varphi, 2\pi)$, and $w^{r,a}(\lambda, \varphi, 2\pi)$ along the meridian $\lambda = \pi$ where the observations are located, for $d_2 = 1$ and $\sigma^2 = 31$ (Fig. 3) and for $d_2 = 0.1$ and $\sigma^2 = 3$ (Fig. 4). These values of σ^2 were chosen by running the traditional filter for a discrete set of values of $\sigma^2 \in [0, 100]$ in increments of $\Delta\sigma^2 = 1$ and then choosing the value of σ^2 for which the trace of P^{rr} is the smallest at time $t = 2\pi$ and for which the trace of P^{rr} is also smaller than the trace of S^{rr} throughout the assimilation period up to $t = 10\pi$. It is evident by comparing the full-state w and the resolved-scales-state w^r in Fig. 3 (left panel) that for $d_2 = 1$ the observation error due to unresolved scales is large, while for $d_2 = 0.1$ (Fig. 4, left panel) it is modest. The corresponding state estimates $w^{r,a}$ have different phases compared to w^r, and in the case of $d_2 = 1$ even the amplitude of $w^{r,a}$ is significantly different from that of w^r. The right panels in Figs. 3 and 4 show the trace of the computed and actual covariance functions. From these tests we conclude that the unresolved-scales covariance between observation locations must be modeled more carefully when the observation error due to unresolved scales is large.

Additional experiments, holding the approximate unresolved-scales covariance matrix constant in time but not necessarily diagonal, also gave unsatisfactory results (not shown). In one set of experiments, $\mathbf{H}^c_{2k}[\mathbf{H}^c_{1k}W^{uu}(\cdot, \cdot, t_k)]^{\mathrm{T}}$ was approximated by the zero matrix, thus ignoring the observation error due to unresolved scales entirely. In another set, $\mathbf{H}^c_{2k}[\mathbf{H}^c_{1k}W^{uu}(\cdot, \cdot, t_k)]^{\mathrm{T}}$ was approximated by its value at time $t = \pi$. From these experiments we conclude that accounting for the time dependence of the observation error due to unresolved scales is important in our model problem.

A simple time-dependent approximation is to approximate $\mathbf{H}^c_{2k}[\mathbf{H}^c_{1k}W^{uu}(\cdot, \cdot, t_k)]^{\mathrm{T}}$ by its diagonal part, that is, to take $\mathbf{H}^c_{2k}[\mathbf{H}^c_{1k}C^u(\cdot, \cdot)]^{\mathrm{T}} = \mathrm{diag}(\mathbf{H}^c_{2k}[\mathbf{H}^c_{1k}W^{uu}(\cdot, \cdot, t_k)]^{\mathrm{T}}$

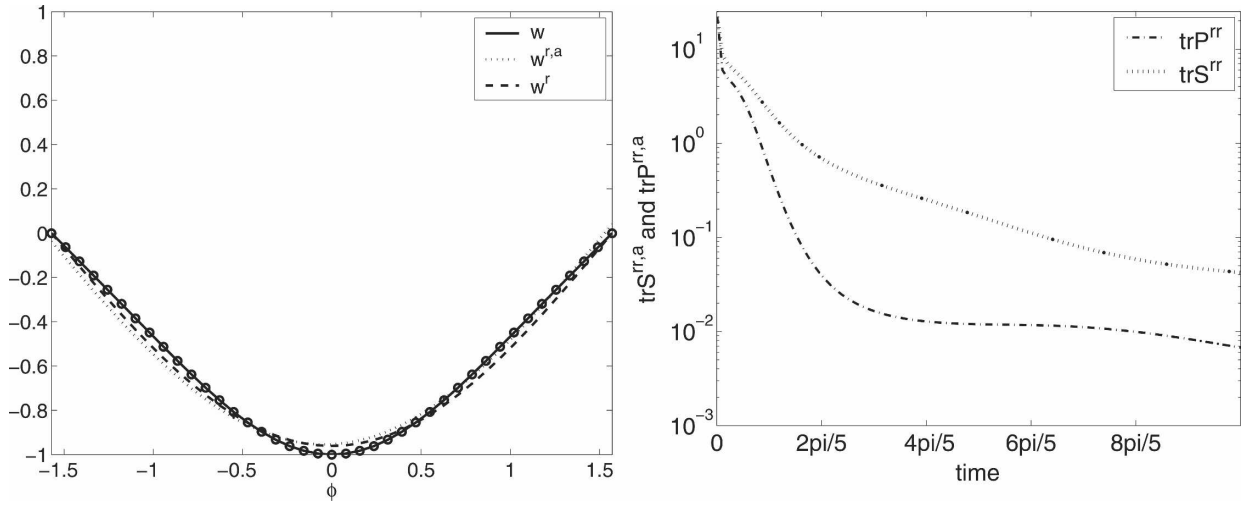

FIG. 4. As in Fig. 3 but for $d_2 = 0.1$ and with $\mathbf{H}^c_{2k}[\mathbf{H}^c_{1k}W^{uu}(\cdot, \cdot, t_k)]^{\mathrm{T}}$ approximated by $3\mathbf{I}$.

at every time t_k. Results under this approximation for the traditional filter with $d_2 = 1$ are shown in Fig. 5. There is now excellent agreement between the state estimate $w^{r,a}$ and the true resolved-scale state w^r, as shown in the left panel of Fig. 5, and this is borne out by the global performance metrics shown in the right panel. However, the computed covariance now underestimates the actual covariance significantly (Fig. 5, right panel). The sudden decrease in trace near 0.7 cycles corresponds to the first zero of the function $j_0(d_2t) + j_2(d_2t)$ in (55). At that time $\hat{w}_{11}(t) = 0$ for all realizations, and we are only estimating $\hat{w}_{10}(0)$.

While the results shown in Fig. 5 are promising, overestimates of the actual estimation error covariance are preferred to underestimates as a general rule (Cohn 1997, p. 267 and p. 268). Furthermore, the approximation of Fig. 5 requires specifying a large number of parameters, one per observation, which is far more than can be estimated reliably in practice (Dee 1995). Therefore, we next consider approximating $\mathbf{H}^c_{2k}[\mathbf{H}^c_{1k}W^{uu}(\cdot, \cdot, t_k)]^{\mathrm{T}}$ by $\sigma_k^2\mathbf{I}$, where $\sigma_k^2 \equiv \mathrm{trace}(\mathbf{H}^c_{2k}[\mathbf{H}^c_{1k}W^{uu}(\cdot, \cdot, t_k)]^{\mathrm{T}})$, since $\mathbf{A} \leq \mathrm{trace}(\mathbf{A})\mathbf{I}$ for every positive semidefinite matrix $\mathbf{A}$; that is, $\mathbf{x}^{\mathrm{T}}\mathbf{A}\mathbf{x} \leq \mathrm{trace}(\mathbf{A})\mathbf{x}^{\mathrm{T}}\mathbf{x}$ for all $\mathbf{x}$. This simple way to overestimate $\mathbf{H}^c_{2k}[\mathbf{H}^c_{1k}W^{uu}(\cdot, \cdot, t_k)]^{\mathrm{T}}$ accounts for its time dependence, and depends on only one parameter, namely σ_k^2.

Global performance results for the traditional filter under this approximation are shown in Fig. 6 for $d_2 = 1$ (left panel) and $d_2 = 0.1$ (right panel). Comparing the left panel in Fig. 6 with the right panel in Fig. 3, and the

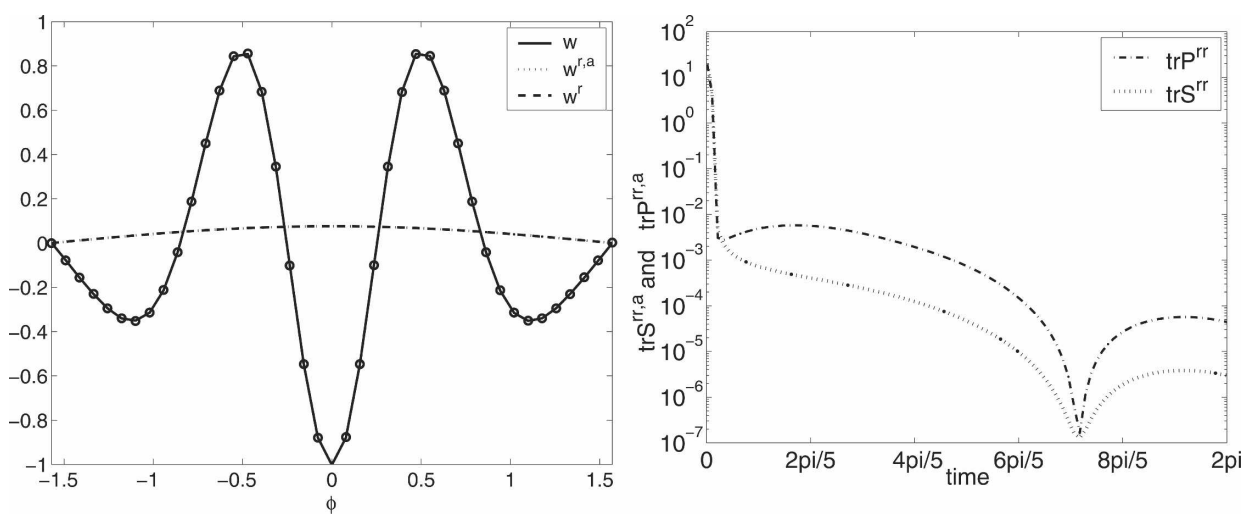

FIG. 5. As in Fig. 3 but with $\mathbf{H}^c_{2k}[\mathbf{H}^c_{1k}W^{uu}(\cdot, \cdot, t_k)]^{\mathrm{T}}$ approximated by $diag(\mathbf{H}^c_{2k}[\mathbf{H}^c_{1k}W^{uu}(\cdot, \cdot, t_k)]^{\mathrm{T}})$.

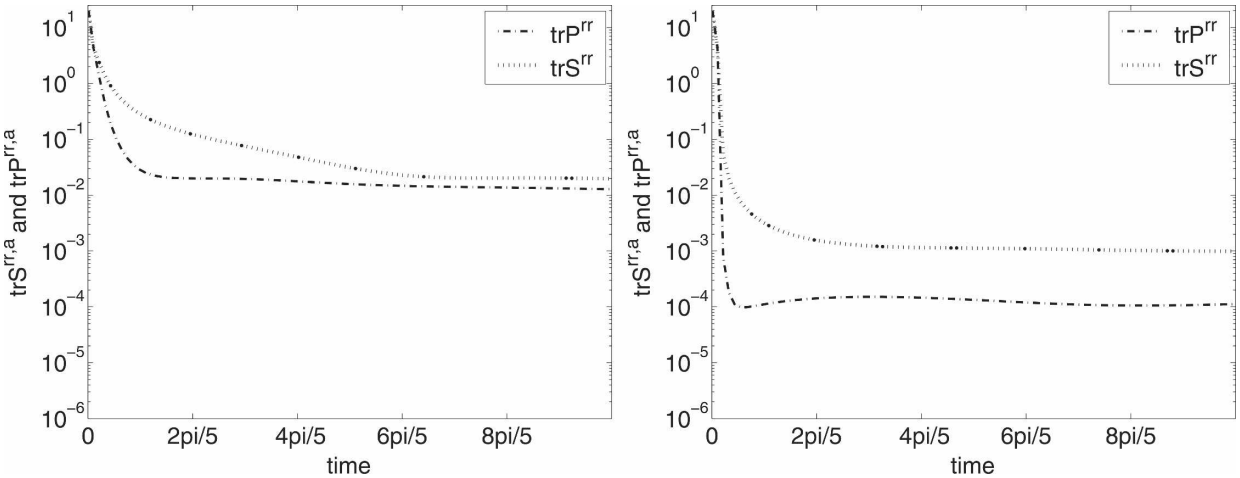

FIG. 6. Comparison of the actual and computed covariances for the traditional filter with $\mathbf{H}^c_{2k}[\mathbf{H}^c_{1k}W^{uu}(\cdot,\cdot,t_k)]^{\mathrm{T}}$ approximated by $\mathrm{trace}(\mathbf{H}^c_{2k}[\mathbf{H}^c_{1k}W^{uu}(\cdot,\cdot,t_k)]^{\mathrm{T}})\mathbf{I}$, for (left) $d_2 = 1$ and (right) $d_2 = 0.1$. The trace of the computed covariance $S^{rr,a}_k$ of the traditional filter is denoted by the dotted line. The trace of the actual covariance $P^{rr,a}_k$ for the traditional filter is represented by the dashed–dotted line. Units are as in Fig. 2. Log scale is used on the ordinate.

right panel in Fig. 6 with the right panel in Fig. 4, we see substantial improvement due to the time dependence of σ^2_k. However, comparing the left panel in Fig. 6 with the right panel in Fig. 5, we see that neglecting the spatial structure along the diagonal of $\mathbf{H}^c_{2k}[\mathbf{H}^c_{1k}W^{uu}(\cdot,\cdot,t_k)]^{\mathrm{T}}$ detracts significantly from performance.

To capture this spatial structure at least crudely, we make use of the inequality $\mathbf{H}^c_{2k}[\mathbf{H}^c_{1k}W^{uu}(\cdot,\cdot,t_k)]^{\mathrm{T}} \le \tau^2_k\mathbf{C}$, where $\mathbf{C}$ is the diagonal matrix whose diagonal elements are $\cos\varphi_i$, φ_i being the observation locations, and where

$$\tau^2_k \equiv \sum_{i=1}^{p_k} \frac{1}{\cos\varphi_i}\{\mathbf{H}^c_{2k}[\mathbf{H}^c_{1k}W^{uu}(\cdot,\cdot,t_k)]^{\mathrm{T}}\}_{ii}. \qquad (63)$$

This inequality, proven in appendix B, is a consequence of the fact that the spherical harmonic coefficients of $W^{uu}(\lambda_1, \varphi_1, \lambda_2, \varphi_2, t)$ are all zero for zonal wavenumber $m = 0$. Global performance results for the traditional filter using the model $\mathbf{H}^c_{2k}[\mathbf{H}^c_{1k}C^u_k(\cdot,\cdot)]^{\mathrm{T}} = \tau^2_k\mathbf{C}$ are shown in Fig. 7 for $d_2 = 1$ (left panel) and $d_2 = 0.1$ (right panel). Significant improvement is seen over the results shown in Fig. 6. In particular, the sharp drop for $d_2 = 1$ near 0.7 time cycles has now returned. The trace of the actual estimation error covariance $P^{rr,a}_k$ for $d_2 = 1$ is, however, about an order of magnitude larger than that for the model of Fig. 5 (right panel). On the other hand, the model in Fig. 7 does result in $S^{rr,a}_k$ overestimating $P^{rr,a}_k$, and in fact it depends on only one

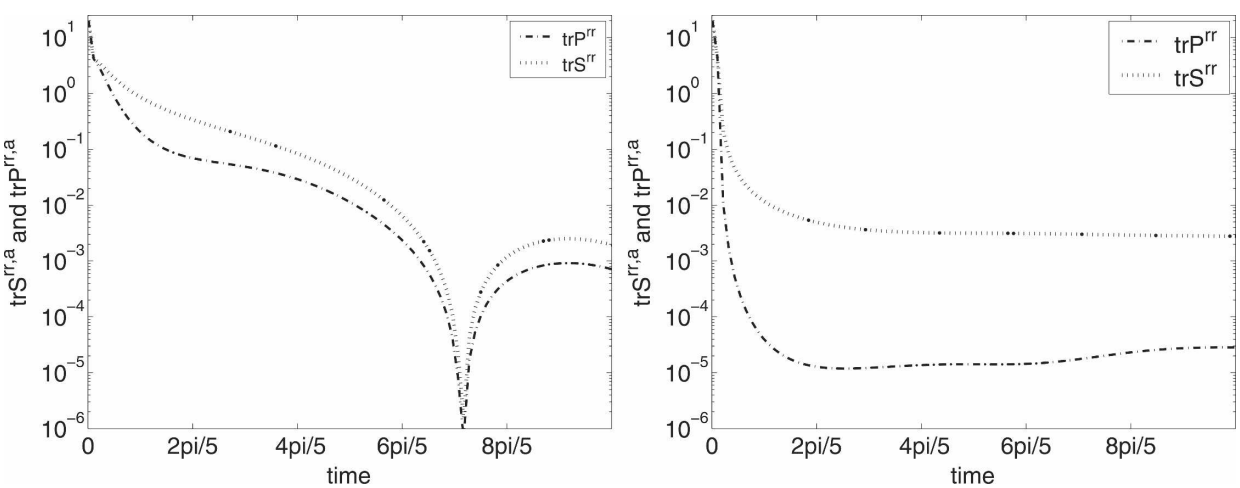

FIG. 7. As in Fig. 6 but with $\mathbf{H}^c_{2k}[\mathbf{H}^c_{1k}W^{uu}(\cdot,\cdot,t_k)]^{\mathrm{T}}$ modeled using $\tau^2_k\mathbf{C}$ (see text for details).

parameter, namely τ_k^2. The possibility of estimating this parameter adaptively, based on the observations themselves rather than on the knowledge of $W^{uu}(\cdot, \cdot, t_k)$ that we have in this model problem, is left to future work.

5. Summary and conclusions

This study has considered the observation error due to unresolved scales in atmospheric data assimilation. Two filter designs to treat this error were derived from the continuum Kalman filter and were tested on a simple model problem. The first of these, a version of the Schmidt–Kalman filter, could be implemented exactly for the model problem. In general this filter requires further approximation, due to the presence of correlation between resolved scales and the unresolved scales, which are infinite in number. It is of theoretical interest, however, because the resolved-scales covariance matrices it calculates are in fact the actual estimation error covariances. The filter formulation of Mitchell and Daley (1997a,b) is also a version of the Schmidt–Kalman filter.

The second filter design resembles the traditional discrete Kalman filter. In principle it can be implemented exactly, in that its evolution equations are defined on a finite-dimensional space. It does not require knowledge of the unresolved-scales covariance function itself, but only of the representativeness error covariance matrix obtained by evaluating this function at the observation locations.

These two filters were tested for the problem of assimilating point observations of a passive tracer in an idealized shear flow on the sphere. This model problem was carefully formulated in such a way as to isolate the observation error due to unresolved scales and to avoid other error sources that are generally present in practice, such as the errors of discretizing the dynamics and the observation operator. For the point observations, the observation error due to unresolved scales was usually large relative to the measurement error, and it increased rapidly with increase of the shear parameter. The unresolved-scales covariance function was also highly anisotropic and nonstationary.

Both filters performed well when supplied with the exact unresolved-scales covariance function. For the traditional filter, diagonal approximations of the representativeness error covariance matrix were also tested. Stationary approximations fared poorly. Approximating this matrix by its diagonal part resulted in much better performance, but the computed resolved-scales covariances in this case underestimated the actual estimation error covariances. Approximating the representativeness error covariance matrix by an appropriate diagonal overestimate of this matrix resulted in good performance, and in computed resolved-scales covariances that overestimate the actual estimation error covariances. The diagonal overestimate depends on a single, time-dependent parameter, which is related to the trace of the representativeness error covariance matrix.

An important implication of these results is that in practice, even when the unresolved-scales covariance function is highly anisotropic and nonstationary, it may still be possible to treat the observation error due to unresolved scales adequately. We obtained good performance results even with a rather crude approximation of the full Kalman filter equations, and very limited information about the unresolved-scales covariance function.

Acknowledgments. This work was funded under the NASA High Performance Computing and Communications Initiative (HPCC) Earth and Space Science (ESS) Program Cooperative Agreement Number NCCS5-150, the NASA EOS Interdisciplinary Science Program, and the NASA Research and Applications Program. Some of this work was performed while the first author held a National Research Council Associateship Award at NASA GSFC. The authors are grateful to Dr. Peter M. Lyster for useful discussions and support in the early stages of this work, and to an anonymous reviewer whose comments were helpful in improving the presentation.

APPENDIX A

Solution of the Advection Equation in Terms of Spherical Harmonics

Lemma 1: If the streamfunction $\Psi = \Psi(\varphi)$ is independent of λ, then for the initial condition given by

$$w(\lambda, \varphi, 0) = \sum_{l=0}^{N} \sum_{m=-l}^{l} \hat{w}_{lm}(0) Y_l^m(\lambda, \varphi), \qquad \text{(A1)}$$

the spherical harmonic coefficients of the solution (54) are zero for $|m| > N$.

Proof: From (A1) using the method of the characteristics it can be shown that the solution of the advection equation for streamfunction independent of λ is given by (see Janjić 2001)

$$w(\lambda, \varphi, t) = \sum_{l=0}^{N} \sum_{m=-l}^{l} \hat{w}_{lm}(0) Y_l^m\left(\lambda + \frac{1}{a^2 \cos\varphi} \frac{\partial \Psi}{\partial \varphi} t, \varphi\right), \qquad \text{(A2)}$$

and due to the orthogonality of the spherical harmonics, from (54) and (A2) we get

$$\hat{w}_{pq}(t) = \sum_{l=0}^{N} \sum_{m=-l}^{l} \hat{w}_{lm}(0) A_{lm} A_{pq} \int_{-\pi/2}^{\pi/2} P_l^{|m|}(\sin\varphi) P_p^{|q|}(\sin\varphi) e^{(iq/a^2 \cos\varphi)(\partial\Psi/\partial\varphi)t} \cos\varphi \, d\varphi \int_0^{2\pi} e^{i(m-q)\lambda} \, d\lambda. \tag{A3}$$

From (A3) we see that $\hat{w}_{pq}(t) = 0$ unless $m = q$, and since $|m| \leq N$, then

$$\hat{w}_{pq}(t) = 0, \quad \forall |q| > N. \tag{A4}$$

Lemma 2: If $l_1 + l_2 + l_3 + |m_1| + |m_2| + |m_3|$ is odd, or if $|m_1| + |m_2| + |m_3|$ is even and $|l_1 - l_3| > l_2$, or if $|m_1| + |m_2| + |m_3|$ is even and $l_2 > l_1 + l_3$, then

$$\int_{-1}^{1} P_{l_1}^{|m_1|}(x) P_{l_2}^{|m_2|}(x) P_{l_3}^{|m_3|}(x) \, dx = 0.$$

Proof: First, note that the associated Legendre function $P_l^{|m|}(x)$ can be written as

$$P_l^{|m|}(x) = (1 - x^2)^{|m|/2} Q_{l-|m|}(x). \tag{A5}$$

Here, $Q_{l-|m|}(x)$ is a polynomial of degree $l - |m|$ with the property that if $l - |m|$ is odd (even), then $Q_{l-|m|}(x)$ is a linear combination of monomials of odd (even) degrees in x. Using (A5) we see that

$$\int_{-1}^{1} P_{l_1}^{|m_1|}(x) P_{l_2}^{|m_2|}(x) P_{l_3}^{|m_3|}(x) \, dx = \int_{-1}^{1} (1 - x^2)^{(|m_1| + |m_2| + |m_3|)/2} Q_{l_1 - |m_1|}(x) Q_{l_2 - |m_2|}(x) Q_{l_3 - |m_3|}(x) \, dx.$$

The product $Q_{l_1-|m_1|}(x) Q_{l_2-|m_2|}(x) Q_{l_3-|m_3|}(x)$ is a polynomial of degree $l_1 + l_2 + l_3 - (|m_1| + |m_2| + |m_3|)$. This degree is odd if $l_1 + l_2 + l_3 + |m_1| + |m_2| + |m_3|$ is odd since it is equal to $l_1 + l_2 + l_3 + |m_1| + |m_2| + |m_3| - 2(|m_1| + |m_2| + |m_3|)$. Therefore, either one or all three of $l_i - |m_i|$ in $Q_{l_1-|m_1|}(x) Q_{l_2-|m_2|}(x) Q_{l_3-|m_3|}(x)$ are odd. Since $Q_{l-|m|}(x)$ is a linear combination of monomials of odd (even) degrees in x, in both of these cases $Q_{l_1-|m_1|}(x) Q_{l_2-|m_2|}(x) Q_{l_3-|m_3|}(x)$ is an odd function. Therefore, in (A5) we are integrating an odd function over a symmetric interval and this integral is zero.

Suppose $l_2 > l_1 + l_3$, then integrating by parts $|m_2|$ times gives

$$\begin{aligned} \int_{-1}^{1} P_{l_1}^{|m_1|}(x) P_{l_2}^{|m_2|}(x) P_{l_3}^{|m_3|}(x) \, dx &= \int_{-1}^{1} (1 - x^2)^{(|m_1| + |m_2| + |m_3|)/2} Q_{l_1 - |m_1|}(x) Q_{l_3 - |m_3|}(x) \frac{d^{|m_2|} P_{l_2}^0(x)}{d^{|m_2|} x} \, dx \\ &= \int_{-1}^{1} \frac{d^{|m_2|}[(1 - x^2)^{(|m_1| + |m_2| + |m_3|)/2} Q_{l_1 - |m_1|}(x) Q_{l_3 - |m_3|}(x)]}{d^{|m_2|} x} P_{l_2}^0(x) \, dx. \end{aligned} \tag{A6}$$

Because $|m_1| + |m_2| + |m_3|$ is even, the expression

$$\frac{d^{|m_2|}[(1 - x^2)^{(|m_1| + |m_2| + |m_3|)/2} Q_{l_1 - |m_1|}(x) Q_{l_3 - |m_3|}(x)]}{d^{|m_2|} x} \tag{A7}$$

is a polynomial of degree $l_1 + l_3$. This polynomial can be written in terms of Legendre polynomials of degree smaller than or equal to $l_1 + l_3$. Therefore, (A6) becomes

$$\int_{-1}^{1} P_{l_1}^{|m_1|}(x) P_{l_2}^{|m_2|}(x) P_{l_3}^{|m_3|}(x) \, dx = \int_{-1}^{1} \sum_{n=0}^{l_1 + l_3} a_n P_n^0(x) P_{l_2}^0(x) \, dx = 0 \tag{A8}$$

due to the orthogonality of Legendre polynomials.

Theorem 1: The solution $w(\lambda, \varphi, t)$ of the advection equation with the streamfunction given by (45), and the initial conditions (48), can be expanded in terms of the spherical harmonics in a series with the coefficients

$$\begin{aligned} &\hat{w}_{l0}(t) = \hat{w}_{l0}(0), \quad \text{for} \quad l \geq 0, \\ &\hat{w}_{l1}(t) = \hat{w}_{11}(0) e^{id_1 t} \frac{A_{11}}{A_{l1}} i^{(l-1)} [j_{l-1}(d_2 t) + j_{l+1}(d_2 t)], \quad \text{for} \\ &\qquad l \geq 1, \\ &\hat{w}_{l,-1}(t) = -\overline{\hat{w}_{l1}(t)}, \quad \text{for} \quad l \geq 1, \\ &\hat{w}_{lm}(t) = 0, \quad \text{for} \quad l \geq |m| \geq 2, \end{aligned} \tag{A9}$$

where j_i for $i = 0, 1, \ldots,$ are the spherical Bessel functions.

Proof: In lemma 1 we proved that for any purely zonal wind, that is, for Ψ independent of λ, and for any initial condition (A1), the number of spherical harmonics of the solution (47) in the zonal direction is not larger than in the initial condition. For the streamfunction (45), using (A1) and (47),

$$w(\lambda,\varphi,t) = \sum_{l=0}^{N} \sum_{m=-l}^{l} \hat{w}_{lm}(0) Y_l^m(\lambda + d_1 t + d_2 \sin\varphi t, \varphi), \tag{A10}$$

and due to the orthogonality of the spherical harmonics it follows that

$$\hat{w}_{pq}(t) = \sum_{l=q}^{N} \hat{w}_{lq}(0) e^{iqd_1 t} 2\pi A_{lq} A_{pq} \times \int_{-1}^{1} P_l^{|q|}(x) P_p^{|q|}(x) e^{iqd_2 xt}\, dx, \ \forall |q| \le N. \tag{A11}$$

Using in (A11) the formula (see Arfken 1995)

$$e^{iqd_2 tx} = \sum_{n=0}^{\infty} i^n (2n+1) j_n(qd_2 t) p_n^0(x) \quad \forall q \le N, q \ge 0, \tag{A12}$$

we get

$$\hat{w}_{pq}(t) = \sum_{l=q}^{N} \sum_{n=0}^{\infty} \hat{w}_{lq}(0) e^{iqd_1 t} 2\pi A_{lq} A_{pq} i^n (2n+1) j_n(qd_2 t) \times \int_{-1}^{1} P_l^{|q|}(x) P_p^{|q|}(x) P_n^0(x)\, dx \ \forall |q| \le N, q \ge 0. \tag{A13}$$

The integral in (A13) vanishes unless $n + l + p$ is even and $|p - l| \le n \le p + l$ (see lemma 2).

Therefore,

$$\hat{w}_{pq}(t) = \sum_{l=q}^{N} \sum_{n=|p-l|}^{p+l} \hat{w}_{lq}(0) e^{iqd_1 t} 2\pi A_{lq} A_{pq} i^n (2n+1) j_n(qd_2 t) \times \int_{-1}^{1} P_l^{|q|}(x) P_p^{|q|}(x) P_n^0(x)\, dx \ \forall |q| \le N, q \ge 0. \tag{A14}$$

In the special case of $q = 0$, $j_n(0) = 0$ for all $n \neq 0$, and $j_0(0) = 1$, so that

$$\hat{w}_{p0}(t) = \hat{w}_{p0}(0) 2\pi A_{p0}^2 \int_{-1}^{1} P_p^0(x) P_p^0(x) P_0^0(x)\, dx = \hat{w}_{p0}(0), \tag{A15}$$

since $P_0^0(x) = 1$ and $\int_{-1}^{1} P_p^0(x) P_p^0(x)\, dx = (2\pi A_{p0}^2)^{-1}$. In the initial condition (50) only the spherical harmonic coefficients $\hat{w}_{10}(0)$, $\hat{w}_{11}(0)$ and $\hat{w}_{1,-1}(0)$ are different from zero. However, we will prove that for all l and all $t > 0$, $\hat{w}_{l1}(t) \neq 0$ for $d_2 \neq 0$. Namely, using (A14),

$$\hat{w}_{p1}(t) = \sum_{n=p-1}^{p+l} \hat{w}_{11}(0) e^{id_1 t} 2\pi A_{11} A_{p1} i^n (2n+1) j_n(d_2 t) \times \int_{-1}^{1} P_1^1(x) P_p^1(x) P_n^0(x)\, dx. \tag{A16}$$

Using lemma 2, and because

$$\int_{-1}^{1} P_1^1(x) P_p^1(x) P_{p-1}^0(x)\, dx = \frac{4p!(p+1)!(2p-2)!}{(p-1)!(2p+1)!(p-1)!} = \frac{2p(p+1)}{(2p+1)(2p-1)}, \tag{A17}$$

and

$$\int_{-1}^{1} P_1^1(x) P_p^1(x) P_{p+1}^0(x)\, dx = \frac{-4(p+1)!(p+1)!(2p)!}{(p-1)!(2p+3)!p!} = \frac{-2p(p+1)}{(2p+1)(2p+3)}, \tag{A18}$$

(A16) becomes

$$\hat{w}_{p1}(t) = \hat{w}_{11}(0) e^{id_1 t} 2\pi A_{11} A_{p1} i^{(p-1)} \frac{2p(p+1)}{2p+1} \times [j_{p-1}(d_2 t) + j_{p+1}(d_2 t)], \tag{A19}$$

that is,

$$\hat{w}_{p1}(t) = \hat{w}_{11}(0) e^{id_1 t} \frac{A_{11}}{A_{p1}} i^{(p-1)} [j_{p-1}(d_2 t) + j_{p+1}(d_2 t)]. \tag{A20}$$

We can obtain the formulas for $\hat{w}_{p,-1}(t)$ from (A20) by noting that for the solution to be real valued we need that

$$-\mathrm{Re}(\hat{w}_{l1}(t)) = \mathrm{Re}(\hat{w}_{l,-1}(t)), \tag{A21}$$

$$\mathrm{Im}(\hat{w}_{l1}(t)) = \mathrm{Im}(\hat{w}_{l,-1}(t)). \tag{A22}$$

APPENDIX B

Bound on the Unresolved-Scales Covariance Function

First we establish the inequality

$$\int_{-\pi/2}^{\pi/2} \int_{-\pi/2}^{\pi/2} f(\varphi_1) V(\varphi_1, \varphi_2, t) f(\varphi_2) \cos\varphi_1 \cos\varphi_2\, d\varphi_1\, d\varphi_2 \le \int_{-\pi/2}^{\pi/2} V(\varphi, \varphi, t) \cos\varphi\, d\varphi \int_{-\pi/2}^{\pi/2} f^2(\varphi) \cos\varphi\, d\varphi \tag{B1}$$

for all functions $f(\varphi)$ that are square integrable against $\cos\varphi$ on $[-\pi/2, \pi/2]$, where

$$V(\varphi_1, \varphi_2, t) \equiv \frac{W^{uu}(\pi, \varphi_1, \pi, \varphi_2, t)}{\cos\varphi_1 \cos\varphi_2}. \tag{B2}$$

Expanding the unresolved-scales covariance function W^{uu} at the meridian $\lambda = \pi$ in terms of the spherical harmonics, we have

$$W^{uu}(\pi, \varphi_1, \pi, \varphi_2, t) = \sum_{l=2}^{\infty} \sum_{|m|=1} \langle \hat{w}_{lm}(t)\overline{\hat{w}_{l,m}(t)}\rangle A^2_{lm} P^1_l(\sin\varphi_1) P^1_l(\sin\varphi_2), \tag{B3}$$

since from (55) the only nonzero spherical harmonic coefficients have $|m| = 1$. Since each $P^1_l(\sin\varphi) = \cos\varphi\, Q_l(\sin\varphi)$ for a polynomial Q_l of degree $l - 1$, this can be rewritten as

$$V(\varphi_1, \varphi_2, t) = \sum_{n=0}^{\infty} \mu_n(t) \sin^n\varphi_1 \sin^n\varphi_2 \tag{B4}$$

for some coefficients $\mu_n(t)$. Equivalently,

$$V(\varphi_1, \varphi_2, t) = \sum_{n=-\infty}^{\infty} \lambda_n(t)\left(\frac{1}{\sqrt{2}} e^{in\pi \sin\varphi_1}\right) \times \left(\frac{1}{\sqrt{2}} e^{-in\pi \sin\varphi_2}\right) \tag{B5}$$

for some coefficients $\lambda_n(t)$, since $\{\sin^n\varphi\}_{n=0}^{\infty}$ and $\{e^{in\pi \sin\varphi}\}_{n=-\infty}^{\infty}$ span the same space, namely the space of functions f such that $\int_{-\pi/2}^{\pi/2} f^2(\varphi) \cos\varphi\, d\varphi$ exists and is finite. Equation (B5) is just an eigenfunction expansion of $V(\varphi_1, \varphi_2, t)$, which can be shown to be a covariance function and therefore has eigenvalues $\lambda_n(t) \geq 0$.

Defining the Fourier coefficients

$$\hat{f}_n \equiv \sqrt{\frac{\pi}{2}} \int_{-\pi/2}^{\pi/2} e^{-in\pi \sin\varphi} f(\varphi) \cos\varphi\, d\varphi \quad \text{and} \tag{B6}$$

$$= \frac{1}{\sqrt{2\pi}} \int_{-\pi}^{\pi} e^{-in\theta} f\left(\sin^{-1}\frac{\theta}{\pi}\right) d\theta, \tag{B7}$$

upon integrating (B5) against $f(\varphi_1)f(\varphi_2) \cos\varphi_1 \cos\varphi_2$ we get

$$\int_{-\pi/2}^{\pi/2} \int_{-\pi/2}^{\pi/2} f(\varphi_1) V(\varphi_1, \varphi_2, t) f(\varphi_2) \cos\varphi_1 \cos\varphi_2\, d\varphi_1\, d\varphi_2 = \frac{1}{\pi} \sum_{n=-\infty}^{\infty} \lambda_n(t) |\hat{f}_n|^2 \quad \text{and} \tag{B8}$$

$$\leq \frac{1}{\pi} \lambda(t) \sum_{n=-\infty}^{\infty} |\hat{f}_n|^2, \tag{B9}$$

where

$$\lambda(t) \equiv \max_{-\infty<m<\infty} \lambda_m(t) \leq \sum_{n=-\infty}^{\infty} \lambda_n(t) = \int_{-\pi/2}^{\pi/2} V(\varphi, \varphi, t) \cos\varphi\, d\varphi. \tag{B10}$$

The final equality in (B10) follows by setting $\varphi_1 = \varphi_2 = \varphi$ and integrating both sides of (B5) against $\cos\varphi$. From Parseval's relation we have

$$\sum_{n=-\infty}^{\infty} |\hat{f}_n|^2 = \int_{-\pi}^{\pi} f^2\left(\sin^{-1}\frac{\theta}{\pi}\right) d\theta = \pi \int_{-\pi/2}^{\pi/2} f^2(\varphi) \cos\varphi\, d\varphi. \tag{B11}$$

Combining (B9), (B10), and (B11) gives (B1).

Now choose $f(\varphi)$ as follows. Define the sets

$$\Phi_i \equiv \left\{\varphi : \varphi \in \left(\varphi_i - \frac{1}{2}\Delta\varphi, \varphi_i + \frac{1}{2}\Delta\varphi\right)\right\}, \quad i = 1, \ldots, p, \tag{B12}$$

where φ_i are the observation locations along the meridian $\lambda = \pi$ and $\Delta\varphi$ is a small number, and let $I_i(\varphi)$ denote the indicator function of Φ_i,

$$I_i(\varphi) \equiv \begin{cases} 1 & \varphi \in \Phi_i \\ 0 & \text{otherwise.} \end{cases} \tag{B13}$$

Given any vector $\mathbf{f} = [f_1, \ldots, f_p]^{\mathrm{T}}$, let

$$f(\varphi) = \frac{1}{\Delta\varphi} \sum_{i=1}^{p} f_i I_i(\varphi). \tag{B14}$$

Inequality (B1) then becomes

$$\mathbf{f}^{\mathrm{T}}\mathbf{W}\mathbf{f} \leq \left(\sum_{i=1}^{p} \eta_i\right) \mathbf{f}^{\mathrm{T}}\mathbf{C}f, \tag{B15}$$

where $\mathbf{W} = \mathbf{W}(t)$ is the matrix whose elements are

$$W_{ij} = \frac{1}{(\Delta\varphi)^2} \int_{\Phi_i} \int_{\Phi_j} W^{uu}(\pi, \varphi_1, \pi, \varphi_2, t)\, d\varphi_1\, d\varphi_2, \tag{B16}$$

$\mathbf{C}$ is the diagonal matrix whose diagonal elements are

$$C_i = \frac{1}{\Delta\varphi} \int_{\Phi_i} \cos\varphi\, d\varphi, \tag{B17}$$

and

$$\eta_i = \eta_i(t) = \frac{1}{\Delta\varphi} \int_{\Phi_i} \frac{W^{uu}(\pi, \varphi, \pi, \varphi, t)}{\cos\varphi}\, d\varphi. \tag{B18}$$

As $\Delta\varphi \to 0$ in (B16)–(B18) at time $t = t_k$ we have

$$W \to \mathbf{H}^c_{2k}[\mathbf{H}^c_{1k}W^{uu}(\cdot,\ \cdot, t_k)]^{\mathrm{T}}, \tag{B19}$$

$$C_i \to \cos\varphi_i, \quad \text{and} \tag{B20}$$

$$\eta_i \to \frac{1}{\cos\varphi_i}(\mathbf{H}^c_{2k}[\mathbf{H}^c_{1k}W^{uu}(\cdot,\ \cdot, t_k)]^{\mathrm{T}})_{ii}, \tag{B21}$$

since the integrands in (B16)–(B18) are continuous at each finite time t_k. This proves the desired result.

REFERENCES

Arfken, G. B., 1995: *Mathematical Methods for Physicists.* Academic Press, 1029 pp.

Atlas, R., 1997: Atmospheric observations and experiments to assess their usefulness in data assimilation. *J. Meteor. Soc. Japan,* **75,** 111–130.

Cohn, S. E., 1997: An introduction to estimation theory. *J. Meteor. Soc. Japan,* **75,** 257–288.

Courtier, P., and Coauthors, 1998: The ECMWF implementation of three-dimensional variational assimilation (3D-Var). I: Formulation. *Quart. J. Roy. Meteor. Soc.,* **124,** 1783–1807.

Daley, R., 1991: *Atmospheric Data Analysis.* Cambridge University Press, 457 pp.

——, 1992: The effect of serially correlated observation and model error on atmospheric data assimilation. *Mon. Wea. Rev.,* **120,** 164–177.

——, 1993: Estimating observation error statistics for atmospheric data assimilation. *Ann. Geophys.,* **11,** 634–647.

Dee, D. P., 1995: On-line estimation of error covariance parameters for atmospheric data assimilation. *Mon. Wea. Rev.,* **123,** 1128–1145.

Desroziers, G., O. Brachemi, and B. Hamadache, 2001: Estimation of the representativeness error caused by the incremental formulation of variational data assimilation. *Quart. J. Roy. Meteor. Soc.,* **127,** 1775–1794.

Gaspari, G., and S. E. Cohn, 1999: Construction of correlation functions in two and three dimensions. *Quart. J. Roy. Meteor. Soc.,* **125,** 723–757.

Hamill, T. M., and J. S. Whitaker, 2005: Accounting for the error due to unresolved scales in ensemble data assimilation: A comparison of different approaches. *Mon. Wea. Rev.,* **133,** 3132–3147.

Janjić, T., 2001: Error due to unresolved scales in estimation problems for atmospheric data assimilation. Ph.D. thesis, University of Maryland, 163 pp.

Jazwinski, A. H., 1970: *Stochastic Processes and Filtering Theory.* Academic Press, 376 pp.

Kalman, R. E., 1960: A new approach to linear filtering and prediction problems. *J. Basic Eng.,* **82D,** 35–45.

——, and R. S. Bucy, 1961: New results in linear filtering and prediction theory. *J. Basic Eng.,* **83D,** 95–108.

Liu, Z.-Q., and F. Rabier, 2002: The interaction between model resolution, observation resolution and observation density in data assimilation: A one-dimensional study. *Quart. J. Roy. Meteor. Soc.,* **128,** 1367–1386.

Lorenc, A. C., 1986: Analysis methods for numerical weather prediction. *Quart. J. Roy. Meteor. Soc.,* **112,** 1177–1194.

Lyster, P. M., S. E. Cohn, B. Zhang, L.-P. Chang, R. Ménard, K. Olson, and R. Renka, 2004: A Lagrangian trajectory filter for constituent data assimilation. *Quart. J. Roy. Meteor. Soc.,* **130,** 2315–2334.

Ménard, R., S. E. Cohn, L.-P. Chang, and P. M. Lyster, 2000: Assimilation of stratospheric chemical tracer observations using a Kalman filter. Part I: Formulation. *Mon. Wea. Rev.,* **128,** 2654–2671.

Mitchell, H. L., and R. Daley, 1997a: Discretization error and signal/error correlation in atmospheric data assimilation. (I). All scales resolved. *Tellus,* **49A,** 32–53.

——, and ——, 1997b: Discretization error and signal/error correlation in atmospheric data assimilation. (II). The effect of unresolved scales. *Tellus,* **49A,** 54–73.

Rodgers, C. D., 2000: *Inverse Methods for Atmospheric Sounding: Theory and Practice.* World Scientific, 238 pp.

Williamson, D. L., J. B. Drake, J. J. Hack, R. Jakob, and P. N. Swarztrauber, 1992: A standard test set for numerical approximations to the shallow water equations in spherical geometry. *J. Comput. Phys.,* **102,** 211–224.